Automatic Localization of Optic Disc in Retinal Fundus Image Based on Unsupervised Learning

J. Prakash and B. Vinoth Kumar

Abstract Automated localization of the optic disc is an essential phase in automated retinal imaging system, which are used in determining the effect of diabetic retinopathy and glaucoma at their initial phase. In this chapter an unsupervised learning technique called clustering methods are used in localization of optic disc. The clustering methods like DBSCAN clustering, Hierarchical Clustering, Fuzzy C Mean and K-Mean clustering are used in optic disc localization. The pre-processing techniques like resizing to avoid images high computation requirement, selection of green color band for processing and smoothing using morphological and gaussian blur operator are performed. Then the optic disc is localized by applying clustering methods by filtering the maximum intensity cluster. The performance of clustering methods was evaluated on three publicly available retinal fundus image databases DRIONSDB dataset containing 110 fundus images, DIARETDB1dataset containing 89 fundus images and High-Resolution Fundus dataset containing 45 fundus images for 10 and 20 iterations respectively. Positive Predicted Value, False Discovery Rate, Accuracy, Error rate, F1 Score, Precision and Recall was determined to analyze the performance of clustering methods. The results infer that the performance of clustering techniques on High Resolution Fundus dataset is better than the other datasets.

1 Introduction

Worlds human population is increasing rapidly, with the increasing population the many people are getting affected by eye disease. Many researchers have identified that the major source of the blindness amongst the world population is because of glaucoma. It affects the optic nerve in the human eye by causing loss of vision. It is

J. Prakash (✉)
Department of CSE, PSG College of Technology, Coimbatore, India
e-mail: jpk.cse@psgtech.ac.in

B. Vinoth Kumar
Department of IT, PSG College of Technology, Coimbatore, India
e-mail: bvk.it@psgtech.ac.in

S. Dash et al. (eds.), *Advanced Soft Computing Techniques in Data Science, IoT and Cloud Computing*, Studies in Big Data 89, https://doi.org/10.1007/978-3-030-75657-4_11

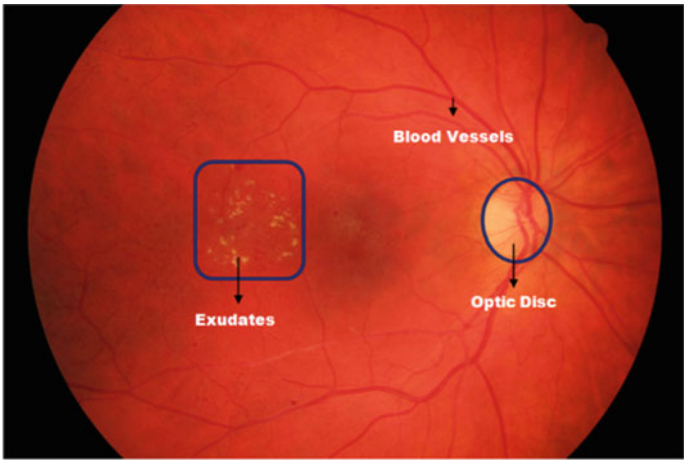

Fig. 1 Structure of fundus image

identified that glaucoma will be severe for the people aged above 40 years and will be very severe for the people aged above 60 years. If the glaucoma is identified at the later stages curing it will become a difficult task. So, the glaucoma is needed to be identified at the earlier stages to control the vision loss. The people will be seen with no symptoms until the human vision get affected which make the detection of eye disease more challenging. The glaucoma can be diagnosed by determining the damage in optic nerve head or by assessing the visual field. Optic disc is a part in the human eye, from where all the optic nerves connect to. It is vertically oval and the dimensions ranging from the average of 1.92 mm vertical dimension and 1.76 mm horizontal dimension [1]. Figure 1 represent the structure of fundus eye image.

The optic disc detection is a vital part of glaucoma diagnosis. In detection of optic disc, the portion of it need to be segmented for glaucoma diagnosis. Optic disc will be varying in sizes and looks bright yellowish color with the blood vessels around it. Cup disc ratio are crucial for diagnosis of disease. The optic disc shall have normal cupping or sometimes they may be flat. Determining the cup disc ratio is an essential part in glaucoma diagnosis. Glaucoma or any other pathology is confirmed if the cup disc ratio is high. If a person is normal and not affected by glaucoma then his vertical cup disc ratio will be lesser than horizontal cup disc ratio. Determining the cup disc ratio is a tedious and laborious process which are done only by the professionals. Automating the optic disc detection may help the diagnosis better, faster and reduce the manual process of detection by experts. In automatic optic disc detection, major parts in retina like blood vessels, optic disc and optic cup looks similar which make the optic disc detection more challenging.

Clustering is an unsupervised method which partitions an image into number of clusters. Agglomerative, Divisive, DBSCAN, OPTICS, Fuzzy C Mean and K-means are some of the clustering methods that can be used for segmenting the

optic disc. The need for localization of optic disc from fundus image is mandatory as they are mostly used by ophthalmologists for human eye diagnosis [2]. Many machine learning techniques were applied in segmentation and localization of optic disc [3]. Also many researchers have experimented the optic disc detection using Evolutionary approaches [4] and deep learning techniques [5, 6]. Partition-based clustering, Density based clustering and Hierarchical based clustering are few unsupervised learning methods, which were used in optic disc localization of fundus image [7, 8].

The objective of this chapter is to determine and localize the optic disc from the fundus image using appropriate clustering methods like DB Scan clustering, Fuzzy C Mean clustering, Hierarchical clustering and K-Means clustering. These clustering methods were applied on the following dataset namely DRIONS DB dataset, DIARETDB1 dataset and High-Resolution Fundus (HRF) dataset. The suitable dataset for the above clustering methods was determined and the performance was analyzed using various performance measures.

The remainder chapter are organized as, the related work is discussed in Sect. 2, followed by discussion about the clustering methods in Sect. 3, Methodology deployed in detecting optic disc in Sect. 4 and Sect. 5 discuss about the results obtained from the clustering algorithms and Sect. 6 about the conclusion.

2 Related Work

Many researches are been carried out in the field of optic disc segmenting in the fundus image. Table 1 summarizes the various approaches in optic disc segmenting of fundus eye image. Lupascu et al. [9] applied a technique for optic disc detection by identifying the finest corresponding circles. In this technique hundreds of circles were generated by providing the initial points and point of interest. The best fitting circles in the optic disc regions are determined using the regression methods and texture descriptors. Based on optimum properties hundreds of circles were reduced to less than twenty circles and the best optic disc circle is determined by selecting the circle in which the correlation coefficient is maximum. This algorithm was tested on the DRIVE dataset containing 40 images and obtained 95% success rate on optic disc localization and 70% for identifying optic disc. Since the images with low quality were not properly detected this technique could be improved.

Youssif et al. [10] applied a matched filter based algorithm for optic disc segmentation called vessels direction matched filter which uses adaptive histogram and illumination equalization for segmenting the retinal blood vessels. In this algorithm, optic disc vessels direction is roughly matched by using the matched filter and the retinal vessels are segmented using 2-D Gaussian matched filter. The optic disc center candidates are then determined by applying low intensity filters to the segmented retinal vessels. The evaluate of proposed algorithm is done by considering the STARE dataset having 81 images and DRIVE dataset containing 40 images and it is determined that the proposed algorithm has correctly identified optic disc center

Table 1 Methods for optic disc segmentation

Author	Optic disc detection technique	Year	Dataset	No of images
Lupascu et al.	Determine best fit circle through noncollinear points	2008	DRIVE	40
Youssif et al.	Vessel direction matched filter	2008	STARE DRIVE	81 40
Zhu and Rangayyan	Hough Transform	2008	DRIVE STARE	40 81
Lu	Circular transformation	2011	STARE ARIA MESSIDOR	81 120 1200
Welfer et al.	Optic disc location vessels arcade information and optic disc boundary using watershed transform	2010	DRIVE DIARETDB1	40 89
Yin et al.	Hough transform and statistical deformable mode	2011	ORIGA	650
Cheng et al.	PPA elimination	2011	ORIGA	650
Tjandrasa et al.	Hough transform to detect circle and active contours to obtain boundary	2012	DRIVE	40
Fraga et al.	Hough transform and Fuzzy convergence	2012	VARIA	120
Zhang et al.	Characteristics of vessel distribution	2012	STARE DRIVE DIARETDB0 DIARETDB1	81 40 130 89

in 80 fundus images (98.77%) in STARE dataset and 40 images (100%) in DRIVE dataset. The future work of the algorithm aims in applying pre-processing techniques in blood vessel segmentation.

Zhu and Rangayyan [11] applied a method using Hough transform for segmenting the optic disc automatically from fundus image, where the detection of edges is done through sobel operators and canny edge detection followed by detection of circles through Hough transform. Color component of the image was normalized as a pre-processing step and morphological erosion to remove the artifacts. The outliers are removed using median filter. Convolving the pre-processed image with specified operators, vertical gradient and horizontal gradient components of the Sobel operator are attained. Canny operators were applied to determine the edges based on optimization procedures, multiscale analysis and multidirectional derivatives. Once the edges were detected the center and radius of the circle was determined by applying Hough transform. DRIVE dataset and STARE dataset are used in testing the algorithm. The algorithm for sobel method achieved a success rate of 40.24% in STARE dataset and 92.5% in DRIVE dataset and a success rate of 80% in DRIVE dataset and

21.95% in STARE dataset for canny method. By applying additional characteristics of optic disc this algorithm can be improved.

Lu [12] proposed a circular transformation technique to determine and segment the optic disc which detects the color variants and circular boundary. In pre-processing the image intensity is determined from the green component and red components which provides more structural information on optic disc. The image was resized to one third and median filter applied to remove noise on blood vessels. Circular transformation is designed by determined the varying distance within the boundary area points and circular area which reaches minimum when the point lies on centroid region. Maximum variation pixels were filtered and by converting the image optic disc map is determined. The maximum values that are present in the optic disc map will represent the optic disc center. MESSIDOR dataset, ARIA dataset, STARE dataset containing 1200, 120, 81 images respectively are considered for evaluating the proposed technique. The optic disc detection accuracy of this technique was found to be 98.77% for MESSIDOR dataset, 99.75 for STARE dataset and 97.5% for ARIA dataset and the accuracy of optic disc segmentation of 93.4% for STARE dataset and 91.7% for ARIA datasets.

Welfer et al. [13] applied an adaptive method to optic disc segmenting the using mathematical morphology, which is robust for the images acquired from varying illumination and acquisition conditions. This methodology has two stages of optic disc detection. Initially the location of optic disc is detected from the vessels arcade information by determining the background and foreground of green channel image using RMIN operator. Next stage the boundary of optic disc is determined using watershed transform. The evaluation was done on DRIVE data set containing 40 images and DIARETDB1 dataset containing 89 images. It achieves a success rate in optic disc localization of DIARETDB1 dataset is 97.75% and DRIVE dataset is 100%. The future works of this work shall consider retina structures like fovea for optic disc detection.

Yin et al. [14] applied a technique which uses circular statistical deformable model, Hough transform and edge detection to determine the optic disc. In pre-processing the effect of blood vessels are reduced by carrying out voting scheme-based heuristics for selection of optimal channel. The optic disc center is determined using Hough transform, while the optic disc boundary is determined using statistical deformable model. Subsequently optic disc circle is approximated using Hough transform and the optic disc center and diameter are determined. Finally, boundaries of image texture are fine-tuned by applying statistical deformable model and optic disc boundary is smoothed by direct least squared ellipse fitting method. The evaluation of the applied technique was determined using ORIGA dataset having 650 images. The result states that this technique have 11.3% average error in the overlapping area and 10.8% average absolute area error.

Cheng et al. [15] applied an elimination method called peripapillary atrophy (PPA) elimination for optic disc segmentation. This proposed method has three stages of implementation include edge filtering, Hough transform and β-PPA detection. In the initial stage the noise is removed by applying low pass filter and the optic disc edges and region of interest are extracted. In edge filtering α and β -PPA was eliminated.

α-PPA includes the epithelial cells which are duskier than the optic disc and β-PPA is similar to the color of optic disc with region of chorioretinal atrophy. α-PPA is determined by comparing the threshold value with the region of interest. Hough transform is applied as the second stage of PPA elimination. In the final stage PPA elimination is to detect β-PPA, due to its similar color as optic disc make the detection difficult when compared to α-PPA. The ring area of optic disc boundary was determined and was segmented into quarters. The feature point is detected by considering the local maxima and minima. The feature points are compared with the threshold, If the feature points are higher than the threshold means than β-PPA is present. The edge points are removed which present along the disc boundary that is detected. The new optic disc boundary is determined by reapplying the constrained elliptical Hough transform. The proposed method is evaluating by considering ORIGA dataset consisting of fundus images. The results infer that the method has 10% average overlapping error, 7.4% average absolute area error and 4.9% average error of vertical disc diameter.

Tjandrasa et al. [16] applied a technique that is initiated by converting the image into grayscale followed by image enhancement using homomorphic filtering to remove the uneven illumination, once the image is enhanced the blood vessels are removed to simplify segmentation task. The low pixel values are determined and the blood vessels are blurred using median filter. The next stage in optic disc segmentation is to perform Hough transform to determine the matched optic disc location. Subsequent optic disc boundaries are determined by performing active contour model. The DRIVE dataset is used for evaluation the experimental results and it found that the optic nerve is segmented with an accuracy of 75.56%.

Fraga et al. [17] applied a model with faster localization and segmentation. This technique uses multiscale retinx algorithm for pre-processing. Fuzzy Hough transform and fuzzy convergence of the blood vessels are used to identify the optic disc location. Optic disc segmentation is then carried out by applying canny filters. Finally, the accuracy of segmentation was determined using histogram information. VARIA dataset containing 120 images is considered for evaluation. The result found that the success rate of proposed algorithm is 100% for optic disc localization and 93.36% for optic disc segmentation.

Zhang et al. [18] used a technique in which the localization is done through 1D projection to determine the optic disc with its appearance characteristic of optic disc in vertical location and vessel distribution of optic disc in horizontal location. The horizontal location of optic disc is determined using vascular degree and with the edge gradients around the optic disc, the vertical location was obtained. In preprocessing the region of interest was identified using mask operation. Once the preprocessing is complete optic disc horizontal location is computed based on vascular degree, then the vascular scatter degree is determined by defining vertical window and sliding over the vessel map. The optic disc vertical location is computed using 1D vertical projection signal which is obtained by defining the rectangular window centered at optic disc horizontal location and sliding over Gabor filter map. Evaluation of proposed algorithm was done by considering the DRIVE dataset containing 40 images, STARE dataset containing 81 images, DIARETDB0 dataset containing 130

images and DIARETDB1 dataset containing 89 images. The outcomes infer that the success rate of DRIVE dataset is 100%, STARE dataset is 91.4%, DIARETDB0 dataset is 95.5% and DIARETDB1 dataset is 92.1%.

3 Clustering Methods

Clustering is broadly used in the area of image segmentation. This clustering methods forms a variety of separate clusters by partitioning the images [19]. The clustering is generally classified as Density based clustering method, Hierarchical based clustering method and Partition based clustering method. Figure 2 represent the complete classification of clustering methods.

Partition method:

It divides the data into number of partitions based on their characteristics and similarity. Once the user specifies the number of partitions to be made the algorithm divides the data into as many partitions, where every partition represents a cluster. Partition clustering methods may include K-Means, K-medoids, CLARA, FCM, etc.

Hierarchical method:

It involves formation of clusters in a planned order, which will be grouping into tree of clusters. Initially it will identify and merge the two comparable clusters which are close to each other and will be continued until all the comparable clusters are combined each other. The major aim of hierarchical clustering method is to generate a hierarchical series of nested cluster. The basic methods of hierarchical clustering include Agglomerative and Divisive clustering methods. Agglomerative clustering

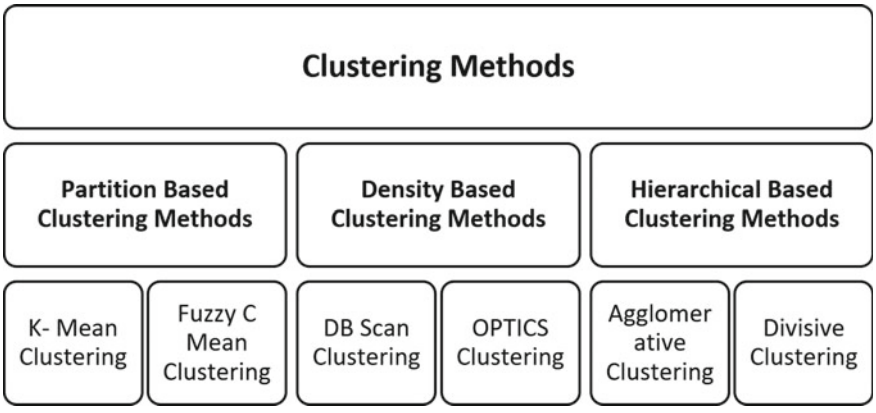

Fig. 2 Classification of clustering methods

method uses an approach which is bottom up while the Divisive which uses the top down approach.

Density based method:

It is a clustering method where the clusters are determined by forming a distinctive cluster one for high density data and another for low density data. Typically, the low-density data are considered as outlier or noise. The different types of density-based methods may include DBScan, Optics, etc.

3.1 Agglomerative Clustering

Agglomerative clustering is a bottom up method of hierarchical clustering in which individual clusters are considered form initial data point. The comparable clusters are joined to other clusters in each iteration until the formation of a cluster.

Agglomerative clustering Algorithm
Determine Matrix
Let the unique Cluster be a Data Point
Repeat until formation of N clusters
Merge the Two Neighboring Clusters.
Update Matrix.

3.2 K-Means Clustering

Most extensively used iterative techniques are K Means clustering that partition the data into discrete non-overlapping clusters with individual data fit into the group. It ensures individual cluster are different by making similar inter-cluster data points. Sum of squared distance between data points are assigned as a cluster to data points [20].

K-Means clustering Algorithm
Input No of cluster (N)
Initialize Centroids by shuffling the dataset
Repeat until centroid does not have any change
Compute data points sum of squared distance
Assign data point to each of the nearby cluster
Determine mean and compute cluster centroids.

3.3 Fuzzy C Mean Clustering

It is an iterative clustering technique where as in fuzzy logic, each point has a grade off fitting to a cluster, rather entirely fitting to a single cluster. Thus, the degree of points on the centre of the cluster will be superior the points on the edge of a cluster. Fuzzy c-means tries partition of a partial group of elements into group of fuzzy clusters with specified condition. It is built on minimization of succeeding objective function [21].

$$J(X, Y) = \sum_{i=1}^{n} \sum_{q=1}^{a} (X_{p,q})^{r} \left|\left| w_p - y_q \right|\right|^2$$

Here,

- r—Real nos > 1.
- a—No of clusters.
- n—No of data.
- $\| w_p - y_q \|$—distance between data point p and present cluster centre q.
- X_{pq}—Membership value.

Fuzzy C Mean Clustering Algorithm
Each cluster are assigned with a random centroid
Repeat until centroid does not have any change.
Determine centroid based on the distance between the cluster center and datapoint.
Centroid is **updated** based on new member function
If new and original centroid distance is lower than threshold
then stop because it is an Epsilon.
else
Continue until the condition becomes true.

3.4 DBSCAN Clustering

Most common density-based clustering is a DBSCAN method. It determines samples of high density and low density, then develops the cluster with samples of high density that are more suitable for data with similar density [22].

DBSCAN Clustering Algorithm
Select a point randomly (P)

Identify all the point (P) reachable Point Density
Continue till the points are processed
If Central Point are P
Cluster are formed.
else boundary point is P
density reachable points are Zero.

4 Methodology

The methodology deployed to detect the optic disc is represented in the block diagram below Fig. 3. The fundus eye image is provided as an input which is resized to reduce computational power and preprocessed by selecting the green color band and smoothing. Once the preprocessing is complete clustering technique is applied to it and optic disc region are masked and the portion of optic disc alone is segmented.

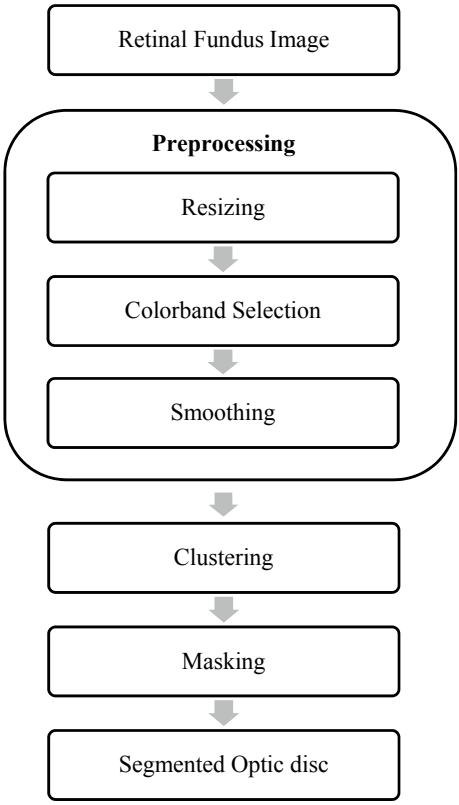

Fig. 3 Process to detecting optic disc

4.1 Retinal Image Pre-processing

The fundus images are given as an input for optic disc detection. The fundus images shall contain different type of noise and may consume more computational capability. To effectively handle those noises and process it effectively the images need to be enhanced by the pre-processing techniques like Resizing, Color band selection and Smoothing [23].

4.1.1 Resizing

The fundus images may be of varying sizes and shall require enormous computational facility and sometimes the images may be too large to fit onto the screen. Thus, the original image is be resized as per the requirement without removing or altering any of its properties. The fundus images in all the dataset are resized to width of 350 and height of 233 (i.e., 350×233).

4.1.2 Color Band Selection

Every pixel is represented either using Red, Green or Blue color with their numeric values ranging from 0 to 255. The colored images may require high computational capability and sometimes does not have pathological structure facts. So, the processing of color image is not a good idea. To overcome this color bands can be separated from the fundus image. The color band which have good contrast is selected for processing the optic disc. In this work it's found that green color band is good and more suitable than blue and red color band.

4.1.3 Smoothing

The green color band fundus image obtained shall comprises of noises and blood vessels. These noises are removed by applying a morphological operator called dilation, which will make improve the images visibility and even fills the small holes that are present in the image then, the high frequency components are removed and the image is made ready for processing by applying gaussian blur operations.

4.1.4 Clustering Methods to Segment Optic Disc

Once the pre-processing of the fundus image is complete, the clustering techniques are applied to determine the optic disc in the fundus image. Clustering method forms a group of clusters by dividing the image into pixels based on their similarities. The

region of optic disc will be having the similar property, so they lie on the single cluster. The optic disc is then segmented from the formed cluster.

4.1.5 Masking

The brightest pixels in the clustered image contains the optic disc. Masking the brightest pixels is needed to determine the optic disc region while the other regions are masked out. A circle of fixed radius is drawn by determining the centroid. The pictorial representation of optic disc segmentation is shown in the Fig. 4.

5 Results and Discussion

5.1 Dataset Description

The algorithm is realized using Open Source Computer Vision Library and is implemented on Intel (R) core i3 processor with a RAM of 4 Giga Bytes. The algorithm was verified with the following publicly available databases like DIARETDB1 dataset,

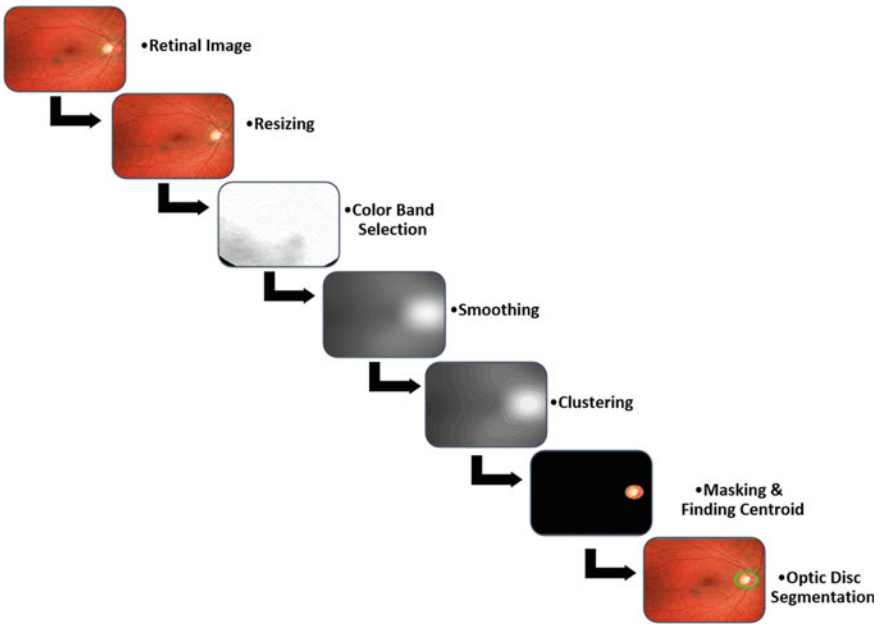

Fig. 4 Pictorial representation of optic disc segmentation in fundus eye image using clustering

Table 2 Dataset description

Dataset	Total images	Healthy images	Unhealthy images	Camera and view of fundus image
HRF	45	15	30	CR-1 fundus camera by canon with 45° view
DIARETDB1	89	05	84	Digital fundus camera with 50° view
DRIONS	110	06	104	Colour analogical fundus camera

DRIONS dataset and High-Resolution Fundus dataset. The detailed description of the three datasets are show in the below Table 2.

5.1.1 High Resolution Fundus Dataset

High Resolution Fundus dataset are available to public usage, which consist of 45 images with an equal spread of 15 fundus images of patients who are healthy, 15 fundus images of patients having diabetic retinopathy and 15 fundus images of patients having glaucomatous. These images are shot on Canon CR-1 fundus camera with 45° view with a resolution of 3304 × 2336 [24].

5.1.2 DIARETDB1 Dataset

DIARETDB1 dataset consist of 89 images with 5 images are considered healthy images and 84 images encompasses mild non-proliferative symptoms considered as unhealthy images. The digital fundus camera was used to shot images with 50° view with a resolution of 1500 × 1152 [25].

5.1.3 DRIONS-DB Dataset

DRIONS-DB is a publicly available dataset consist of 110 images with 6 Healthy images and 104 unhealthy images. These images in this dataset are captured on color analogical fundus camera with a resolution of 600 × 400. [26].

5.2 Result Analysis

Clustering methods K-means clustering, Agglomerative clustering, DBSCAN clustering and Fuzzy C-means clustering techniques performance and accuracy determined and compared on the datasets like HRF, DIARETDB1 and DRIONS datasets.

The optic disc localization by K Means clustering in Figs. 5 and 6, Fuzzy C Means clustering in Figs. 7 and 8, Agglomerative clustering in Figs. 9 and 10 and DBSCAN clustering in Figs. 11 and 12 are shown below. The detected optic disc portion are represented by a green circle.

Figure 13 shows the various stages of optic disc segmenting in fundus image on HRF dataset, DIARETDB1 dataset and DRIONSDB dataset, where the fundus images are given as an input which is been pre-processed by resizing, green channel selection and smoothening. Then the clustering techniques is applied to the processed image by determining and segmenting the optic disc region with a circle.

Figure 14 shows the optic disc segmentation by DBSCAN clustering, Hierarchical clustering, FCM clustering and K Means clustering methods on publicly available databases HRF dataset. The circle in the image represent the optic disc region that is been fittingly segmented by the clustering techniques.

The optic disc segmentation is done by making a circle on the optic disc region on DIARETDB1 dataset by DBSCAN clustering, Hierarchical clustering, FCM clustering and K Means clustering methods is shown in the below Fig. 15.

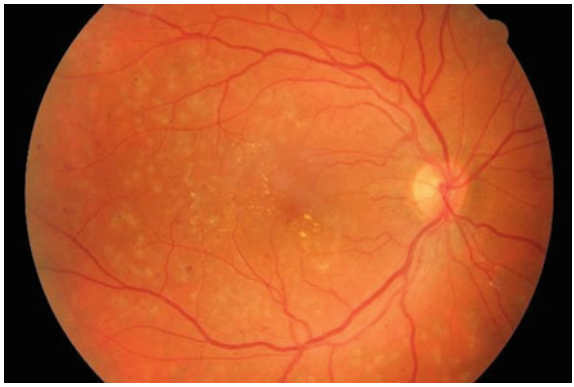

Fig. 5 Input fundus image for DBSCAN clustering

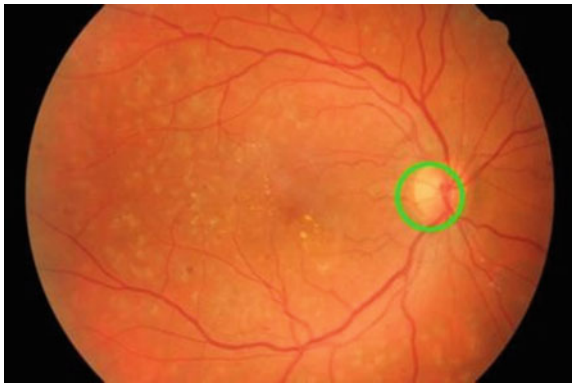

Fig. 6 Localized optic disc by DBSCAN clustering

Fig. 7 Input fundus image for Hierarchical clustering

Fig. 8 Localized optic disc by Hierarchical clustering

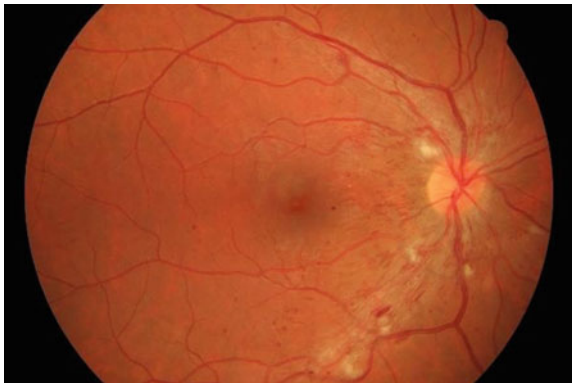

Fig. 9 Input fundus image for FCM clustering

Fig. 10 Localized optic disc by FCM clustering

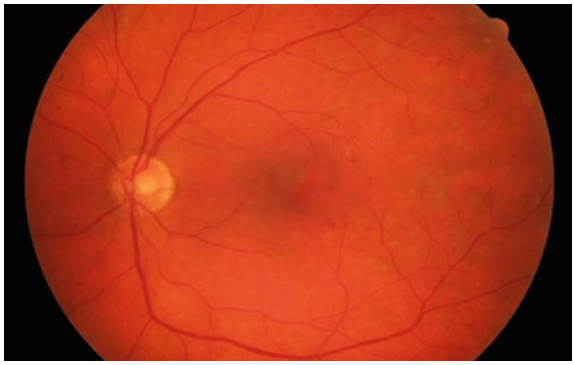

Fig. 11 Input fundus image for K-Means clustering

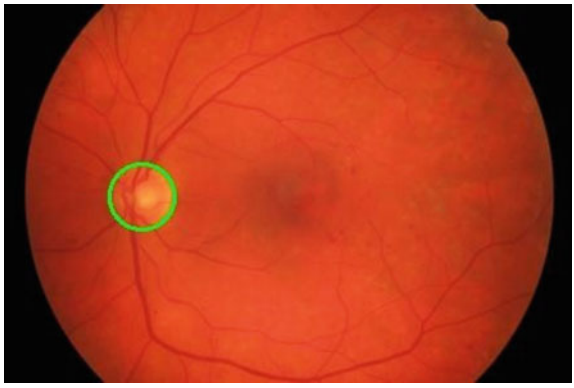

Fig. 12 Localized optic disc by K-Means clustering

Figure 16 shows the sample images of DRIONS dataset where the optic disc is detection and segmentation using DBSCAN, Hierarchical, FCM and K Means clustering techniques. The sample images are taken randomly and be evaluated and displayed in the below figure.

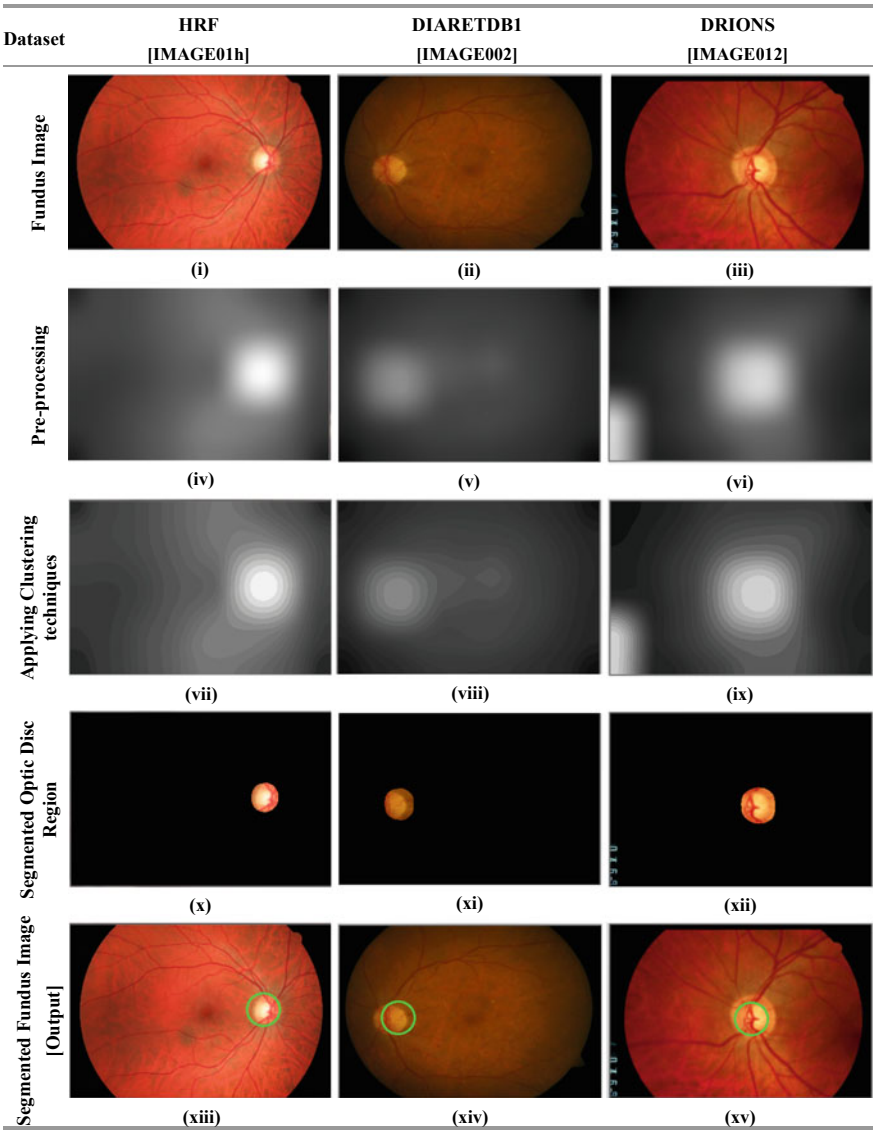

Fig. 13 Stages in segmenting optic disc from fundus image. (i) Input fundus image of HRF dataset, (ii) input fundus image of DIARETDB1 dataset, (iii) input fundus image of DRIONS dataset, (iv) pre-processing of HRF dataset, (v) pre-processing of DIARETDB1 dataset, (vi) pre-processing of DRIONS dataset, (vii) applying clustering technique for HRF dataset, (viii) applying clustering technique for DIARETDB1 dataset, (ix) applying clustering technique for DRIONS dataset, (x) segmented optic disc region of HRF dataset, (xii) segmented optic disc region of DIARETDB1 dataset, (xii) segmented optic disc region of DRIONS dataset, (xiii) output of fundus image in HRF dataset, (xiv) output of fundus image in DIARETDB1 dataset, (xv) output of fundus image in DRIONS dataset

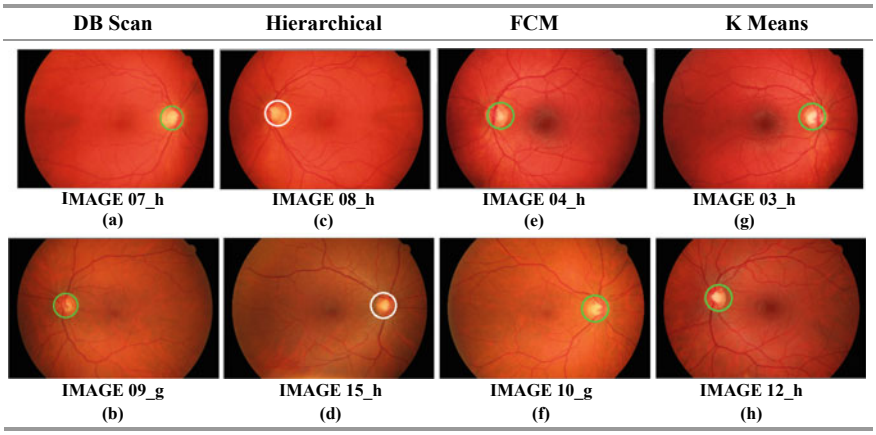

Fig. 14 Examples of correct detection of optic disc on HRF dataset circle represent the segmented region of optic disc. **a** and **b** DBSCAN clustering on HRF dataset, **c** and **d** hierarchical clustering on HRF dataset, **e** and **f** FCM clustering on HRF dataset, **g** and **h** K Means clustering on HRF dataset

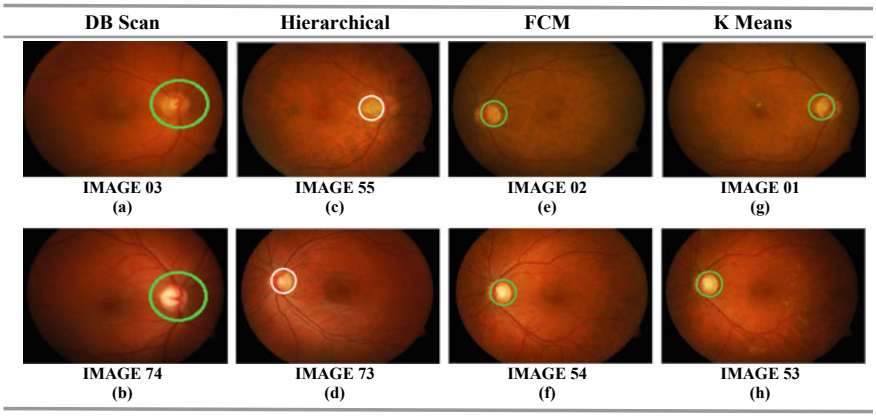

Fig. 15 Examples of correct detection of optic disc on DIARET DB1 dataset circle represent the segmented region of optic disc. **a** and **b** DBSCAN clustering on DIARETDB1 dataset, **c** and **d** hierarchical clustering on DIARETDB1dataset, **e** and **f** FCM clustering on DIARETDB1dataset, **g** and **h** K Means clustering on DIARETDB1dataset

Optic disc segmentation in HRF, DIARETDB1 and DRIONS dataset were done by K Means, Fuzzy C Mean, Hierarchical and DBSCAN clustering techniques. Yet segmentation was non proper in few images because of the image quality. Figure 17 shows some difficult cases in each dataset and in each clustering techniques where the segmentation of optic disc failed.

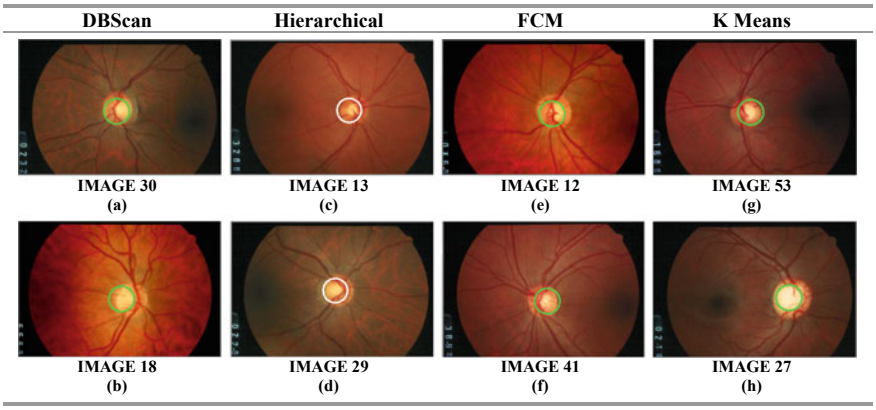

Fig. 16 Examples of correct detection of optic disc on DRIONS dataset circle represent the segmented region of optic disc. **a** and **b** DBSCAN clustering on DRIONS dataset, **c** and **d** hierarchical clustering on DRIONS dataset, **e** and **f** FCM clustering on DRIONS dataset, **g** and **h** K Means clustering on DRIONS dataset

5.3 Optic Disc Detection

The region of optic disc in the fundus image are determined by comparing ground truth centre of the optic disc and manually determined optic disc centre. The detection of optic disc is said to be done (i.e., Hit) if the below equation [19] is fulfilled [4].

$$\sqrt{(A_m - A_d)^2 + (B_m - B_d)^2} < X_{mean}$$

Here, A_m and B_m is manually labelled, A_d and B_d are detected coordinates, X mean denotes the datasets standard average radii. The process is said to be Hit if the equation is satisfied and vice versa if it is a Miss. Table 3 represent the Hit rate determined by applying the clustering algorithms. Figure 18a, b shows the Graphical representation of the clustering techniques on datasets for 10 and 20 iterations.

5.4 Performance Evaluation

The performance measure of detecting optic disc in fundus eye image are determined using various parameters like Positive Predicted Value, False Discovery Rate, Accuracy, F1 Score, Error Rate, Precision and Recall [27], the description of the measure is shown in Table 4. The outcome values of segmented fundus images are determined by evaluating True Positive (TP), False Negative (FN), False Positive (FP) and True Negative (TN) as shown in Fig. 19.

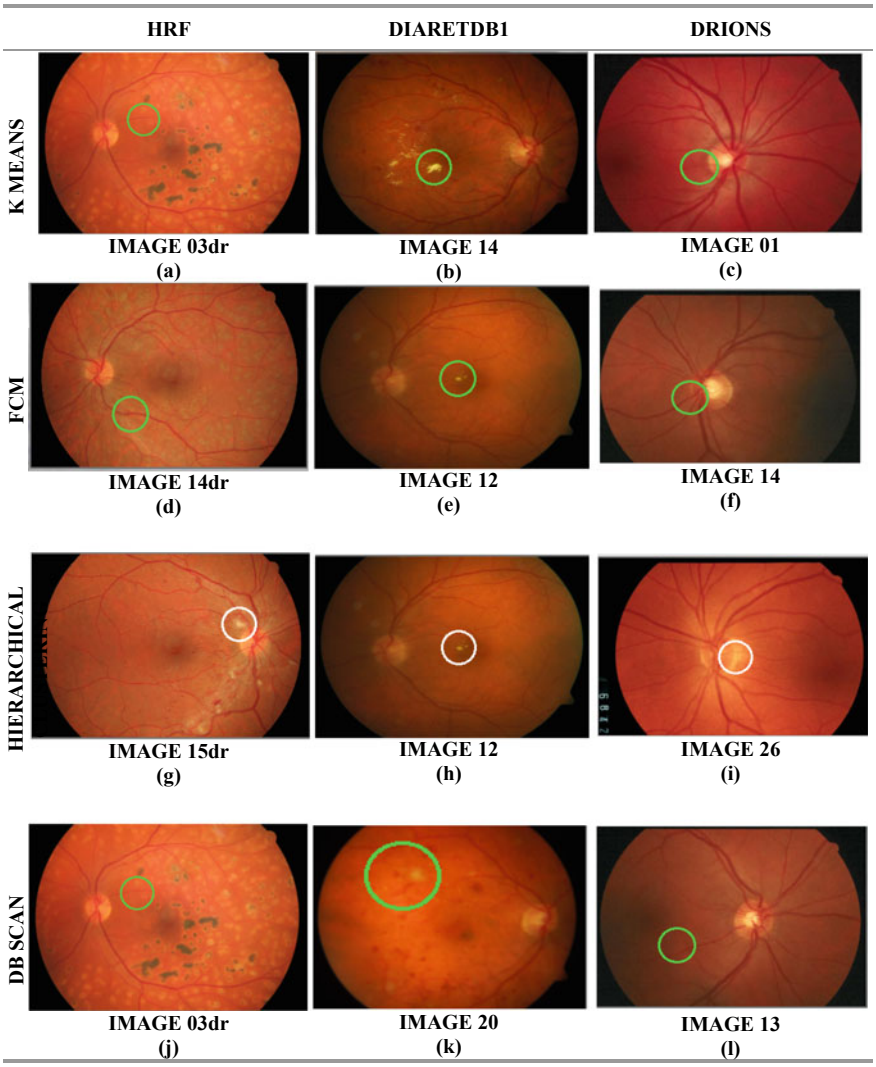

Fig. 17 Incorrect optic disc segmentation in difficult cases. **a** K Means clustering on HRF dataset, **b** K Means clustering on DIARETDB1 dataset, **c** K Means clustering on DRIONS dataset, **d** FCM clustering on HRF dataset, **e** FCM clustering on DIARETDB1 dataset, **f** FCM clustering on DRIONS dataset, **g** hierarchical clustering on HRF dataset, **h** hierarchical clustering on DIARETDB1 dataset, **i** hierarchical clustering on DRIONS dataset, **j** DBSCAN clustering on HRF dataset, **k** DBSCAN clustering on DIARETDB1 dataset, **l** DBSCAN clustering on DRIONS dataset

Table 3 Clustering techniques accuracy

			FCM	DIARETDB1	DRIONS
	No of iteration	**Total images**	45	89	110
K Means	10	Optic disc detection	45	68	82
		Optic disc missed	0	21	28
		Hit rate	**100%**	**76%**	**75%**
	20	Optic disc detection	45	68	85
		Optic disc missed	0	21	25
		Hit rate	**100%**	**76%**	**77%**
FCM	10	Optic disc detection	45	68	78
		Optic disc missed	0	21	32
		Hit rate	**100%**	**76%**	**71%**
	20	Optic disc detection	45	68	74
		Optic disc missed	0	21	36
		Hit rate	**100%**	**76%**	**67%**
Hierarchical	10	Optic disc detection	45	67	110
		Optic disc missed	0	22	0
		Hit rate	**100%**	**75%**	**100%**
	20	Optic disc detection	45	68	110
		Optic disc missed	0	21	0
		Hit rate	**100%**	**76%**	**100%**
DB scan	10	Optic disc detection	45	78	75
		Optic disc missed	0	32	35
		Hit rate	**100%**	**71%**	**68%**
	20	Optic disc detection	45	74	76
		Optic disc missed	0	36	34
		Hit rate	**100%**	**67%**	**69%**

5.5 Discussion

The performance parameters like Positive Predicted Value, False Discovery Rate, Accuracy, Error Rate, Precision and Recall are determined by applying clustering algorithms and identifying True Positive (TP), False Negative (FN), False Positive (FP) and True Negative (FN). The observed result for 10 and 20 iterations are tabulated in the below Table 5 and 6 respectively.

The performance parameters like Positive Predicted Value, False Discovery Rate, Accuracy, Error Rate, Precision and Recall are determined by analyzing clustering techniques for 10 and 20 iterations on HRF dataset and the average values obtained by the techniques on the various performance measures is shown in the below Table 7.

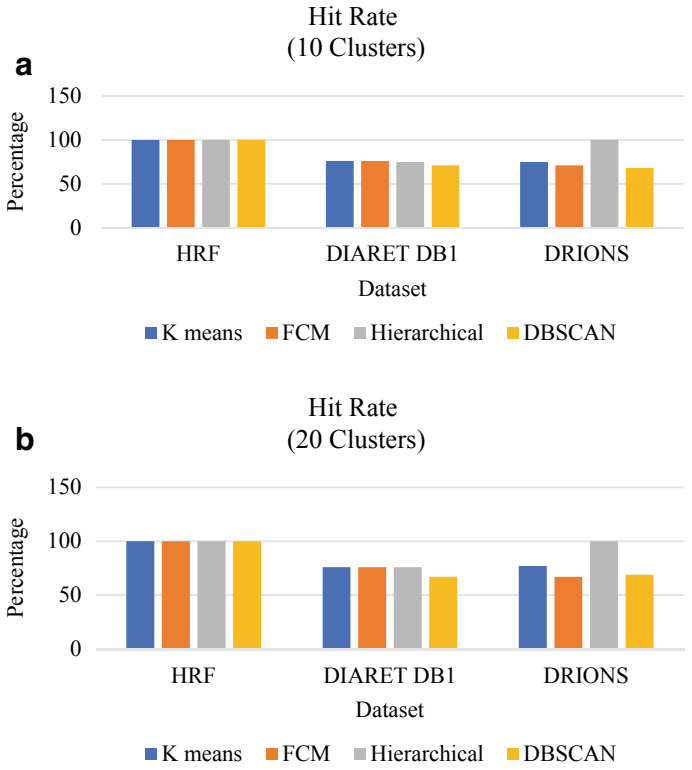

Fig. 18 **a** Hit rate for 10 clusters. **b** Hit rate for 20 clusters

Table 4 Description of performance measure

Measure	Description
Positive predicted value (PPV)	(True Positive)/(False Positive + True Positive)
False discovery rate (FDR)	(False Positive)/(True Positive + False Positive)
Accuracy	(True Positive + True Negative)/Total
Error rate	(False Negative + False Positive)/(False Negative + False Positive + True Negative + True Positive)
F1 score	2 * (Precision * Recall/(Precision + Recall))
Precision	(True Positive)/(True Positive + False Positive)
Recall	(True Positive)/(True Positive + False Negative)

Where,
True Positive (TP) = Correctly detected Optic disc
False Negative (FN) = Unable to detect Optic disc
False Positive (FP) = Optic disc detect but it's incorrectly detected
True Negative (TN) = No Optic Disc No Detection

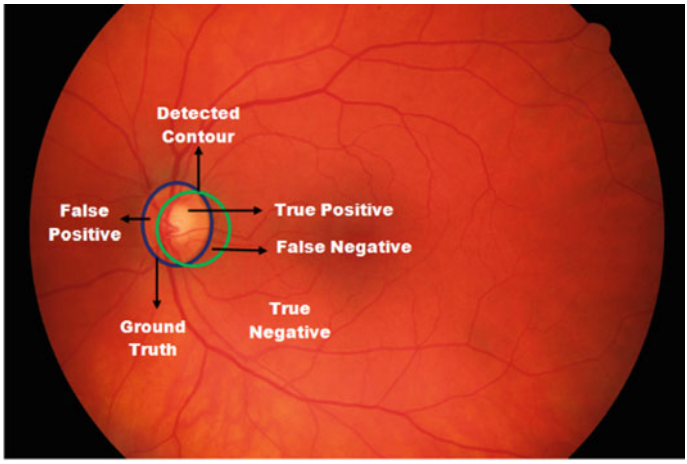

Fig. 19 Determining TP, TN, FP, FN in fundus image

Table 5 Performance measure analysis for 10 iterations

	Dataset	Total images	FP	TP	TN	FN
K means	HRF	45	4	41	0	0
	DIARET DB 1	89	9	59	0	21
	DRIONS	110	8	74	0	28
FCM	HRF	45	1	44	0	0
	DIARET DB 1	89	9	59	0	21
	DRIONS	110	8	70	0	32
Hierarchical	HRF	45	1	44	0	0
	DIARET DB 1	89	5	62	0	22
	DRIONS	110	5	105	0	0
DBSCAN	HRF	45	3	42	0	0
	DIARET DB 1	89	2	42	0	45
	DRIONS	110	1	74	0	35

The performance of the clustering techniques is determined by analysing clustering technique for 10 and 20 iterations on DIARETDB1 dataset and the average values obtained by the techniques on the various performance measures is shown in the below Table 8.

Table 9 represents the result obtained on the DRIONS datasets for 10 iterations and 20 iterations along with the average iteration values by the clustering techniques. Similar to the above results hierarchical clustering technique outperforms others in most of the cases.

Table 6 Performance measure analysis for 20 iterations

	Dataset	Total Images	FP	TP	TN	FN
K Means	HRF	45	2	43	0	0
	DIARET DB 1	89	8	60	0	21
	DRIONS	110	9	76	0	25
FCM	HRF	45	3	42	0	0
	DIARET DB 1	89	8	60	0	21
	DRIONS	110	8	66	0	36
Hierarchical	HRF	45	1	44	0	0
	DIARET DB 1	89	5	63	0	21
	DRIONS	110	4	106	0	0
DBSCAN	HRF	45	4	41	0	0
	DIARET DB 1	89	2	42	0	45
	DRIONS	110	1	75	0	34

Table 7 HRF dataset on clustering techniques

		DB scan clustering	Hierarchical clustering	FCM clustering	K-mean clustering
Precision	Iteration 10	93.33	97.78	97.78	91.11
	Iteration 20	91.11	97.78	93.33	95.56
	Average	92.22	97.78	95.56	93.33
Recall	Iteration 10	100.00	100.00	100.00	100.00
	Iteration 20	100.00	100.00	100.00	100.00
	Average	100.00	100.00	100.00	100.00
Accuracy	Iteration 10	93.33	97.78	97.78	91.11
	Iteration 20	91.11	97.78	93.33	95.56
	Average	92.22	97.78	95.56	93.33
F1 score	Iteration 10	96.55	98.88	98.88	95.35
	Iteration 20	95.35	98.88	96.55	97.73
	Average	95.95	98.88	97.71	96.54
Error rate	Iteration 10	6.67	2.22	2.22	8.89
	Iteration 20	8.89	2.22	6.67	4.44
	Average	7.78	2.22	4.44	6.67
Positive predicted value (PPV)	Iteration 10	0.93	0.98	0.98	0.91
	Iteration 20	0.91	0.98	0.93	0.96
	Average	0.92	0.98	0.96	0.93
False discovery rate (FDR)	Iteration 10	0.07	0.02	0.02	0.09
	Iteration 20	0.09	0.02	0.07	0.04
	Average	0.08	0.02	0.04	0.07

Table 8 DIARETDB1 dataset on clustering techniques

		DB scan clustering	Hierarchical clustering	FCM clustering	K-mean clustering
Precision	Iteration 10	95.45	92.54	86.76	86.76
	Iteration 20	95.45	92.65	88.24	88.24
	Average	95.45	92.59	87.50	87.50
Recall	Iteration 10	48.28	73.81	73.75	73.75
	Iteration 20	48.28	75.00	74.07	74.07
	Average	48.28	74.40	73.91	73.91
Accuracy	Iteration 10	47.19	69.66	66.29	66.29
	Iteration 20	47.19	70.79	67.42	67.42
	Average	47.19	70.22	66.85	66.85
F1 score	Iteration 10	64.12	82.12	79.73	79.73
	Iteration 20	64.12	82.89	80.54	80.54
	Average	64.12	82.51	80.13	80.13
Error rate	Iteration 10	52.81	30.34	33.71	33.71
	Iteration 20	52.81	29.21	32.58	32.58
	Average	52.81	29.78	33.15	33.15
Positive predicted value (PPV)	Iteration 10	0.95	0.93	0.87	0.87
	Iteration 20	0.95	0.93	0.88	0.88
	Average	0.95	0.93	0.88	0.88
False discovery rate (FDR)	Iteration 10	0.05	0.07	0.13	0.13
	Iteration 20	0.05	0.07	0.12	0.12
	Average	0.05	0.07	0.13	0.13

The K-Means clustering method was applied on the DRIONS, DIARETDB1 and HRF dataset for 10 iterations and the results are tabulated in Fig. 20. It is observed from the results that the accuracy of K-Means clustering method on HRF dataset is 91%, which is greater than the other two DIARETDB1 and DRIONS dataset which are have an accuracy of 66% and 67% respectively. Similarly, the K-Means clustering was applied on the DRIONS, DIARETDB1 and HRF dataset for 20 iterations and the obtained results are tabulated in Fig. 21. The result infers that the accuracy of HRF dataset is much better than the other dataset set with HRF dataset having an accuracy of 96% compared to 67% and 69% of DIARETDB1 and DRIONS dataset respectively.

The Performance of hierarchical clustering was determined by applying it on DRIONS, DIARETDB1 and HRF dataset for 10 iteration and the results are tabulated in Fig. 22. With the observation from the results it is inferred that accuracy of hierarchical clustering on HRF dataset is 98% which is greater when compared to the other dataset DIARETDB1 and DRIONS having an accuracy of 70% and 95% respectively. Similarly, Fig. 23 represent the results obtained by performing hierar-

Table 9 DRIONS dataset on clustering techniques

		DB scan clustering	Hierarchical clustering	FCM clustering	K-mean clustering
Precision	Iteration 10	98.67	95.45	89.74	90.24
	Iteration 20	98.68	96.36	89.19	89.41
	Average	98.68	95.91	89.47	89.83
Recall	Iteration 10	67.89	100.00	68.63	72.55
	Iteration 20	68.81	100.00	64.71	75.25
	Average	68.35	100.00	66.67	73.90
Accuracy	Iteration 10	67.27	95.45	63.64	67.27
	Iteration 20	68.18	96.36	60.00	69.09
	Average	67.73	95.91	61.82	68.18
F1 score	Iteration 10	80.43	97.67	77.78	80.43
	Iteration 20	81.08	98.15	75.00	81.72
	Average	80.76	97.91	76.39	81.08
Error rate	Iteration 10	32.73	4.55	36.36	32.73
	Iteration 20	31.82	3.64	40.00	30.91
	Average	32.27	4.09	38.18	31.82
Positive predicted value (PPV)	Iteration 10	0.99	0.95	0.90	0.90
	Iteration 20	0.99	0.96	0.89	0.89
	Average	0.99	0.96	0.89	0.90
False discovery rate (FDR)	Iteration 10	0.01	0.05	0.10	0.10
	Iteration 20	0.01	0.04	0.11	0.11
	Average	0.01	0.04	0.11	0.10

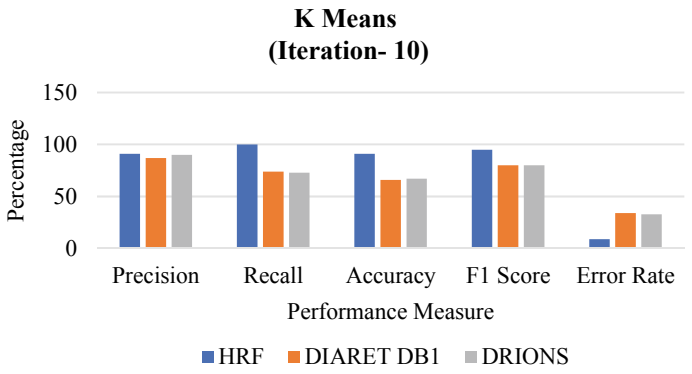

Fig. 20 Performance of K-Means clustering techniques with 10 iterations

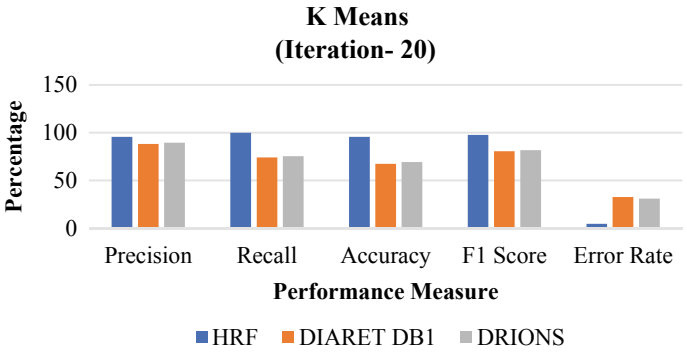

Fig. 21 Performance of K-Means clustering techniques with 20 iterations

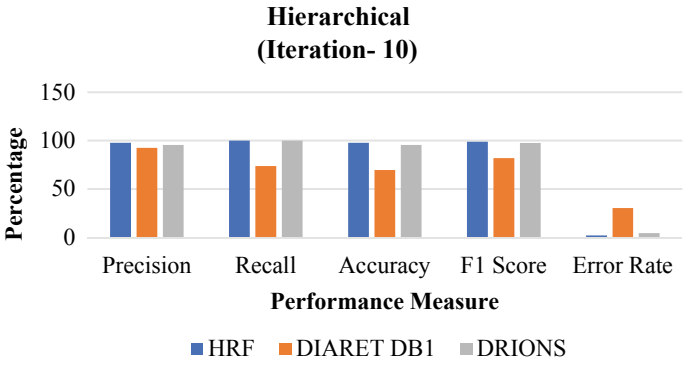

Fig. 22 Performance of hierarchical clustering techniques with 10 iterations

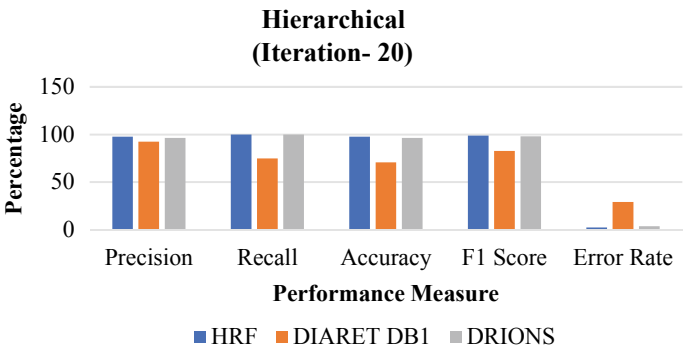

Fig. 23 Performance of hierarchical clustering techniques with 20 iterations

chical clustering on dataset for 20 iterations and the result infer that 98% accuracy on HRF dataset is better than 95% accuracy on DRIONS dataset while the DIARET DB1 dataset have an accuracy of 70% which is less compared to the others datasets.

Fuzzy C Mean clustering was applied on DRIONS, DIARETDB1 and HRF dataset for 10 iteration and 20 iterations respectively. The results obtained from FCM clustering method with 10 iterations is represented in Fig. 24 and for 20 iterations in Fig. 25. The results infer that the performance of HRF data set in both 10 and 20 iterations are better than the other two datasets. The accuracy of HRF dataset for 10 iteration is 98% with comparison to DIARETDB1 and DRIONS with 66% and 64% respectively. While for 20 iterations the 93% accuracy of HRF dataset is better when compared to 67% for DIARETDB1 and 60% for DRIONS dataset.

The Performance of DBSCAN clustering method was determined by applying it on DRIONS, DIARETDB1 and HRF dataset for 10 and 20 iterations. Figure 26 represent the result obtained from DBSCAN clustering method for 10 iterations. It is observed that the accuracy of HRF dataset is 93% which is way better when

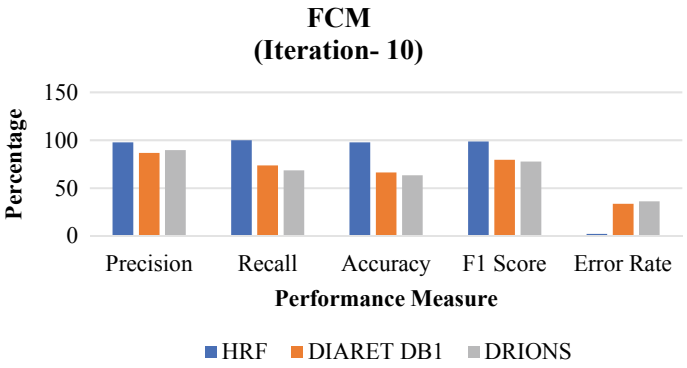

Fig. 24 Performance of FCM clustering techniques with 10 iterations

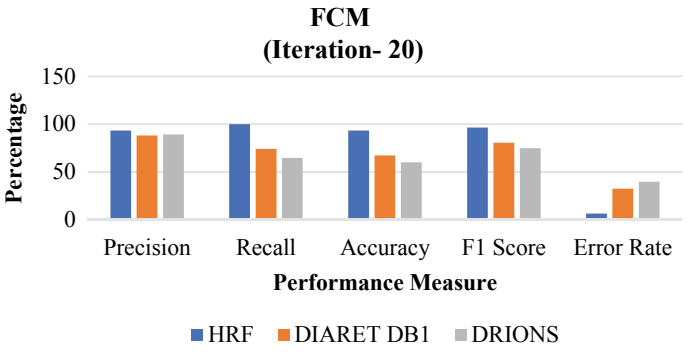

Fig. 25 Performance of FCM clustering techniques with 20 iterations

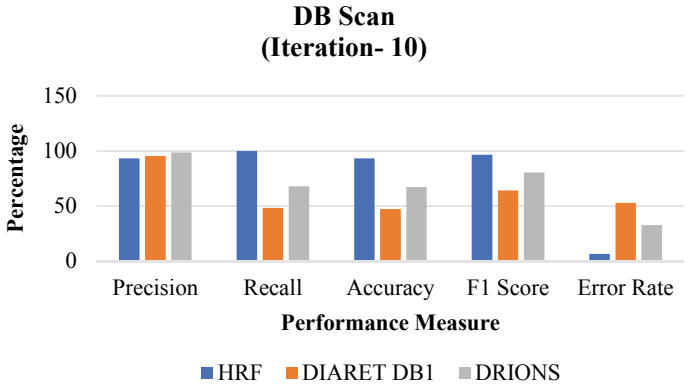

Fig. 26 Performance of DBSCAN clustering techniques with 10 iterations

compared to other DIARETDB1 dataset with 47% and DRIONS dataset with 67%. Similarly, Fig. 27 represent the results obtained by performing DBSCAN clustering on dataset for 20 iterations and the result infer that 91% accuracy on HRF dataset is better than 47% accuracy on DIARETDB1 dataset and 68% accuracy on DRIONS dataset.

The positive predicted values of the clustering algorithms on all the three datasets are determined and is tabulated below. Figures 28 and 29 illustrate that the probability of positively predicted values of hierarchical clustering is better HRF and DIARETDB1 database, while DBSCAN clustering is better in DRIONS dataset for 10 iterations. For 20 iterations the positively predicted values of hierarchical clustering are greater for HRF dataset while DBSCAN clustering is better for DIARETDB1 and DRIONS datasets.

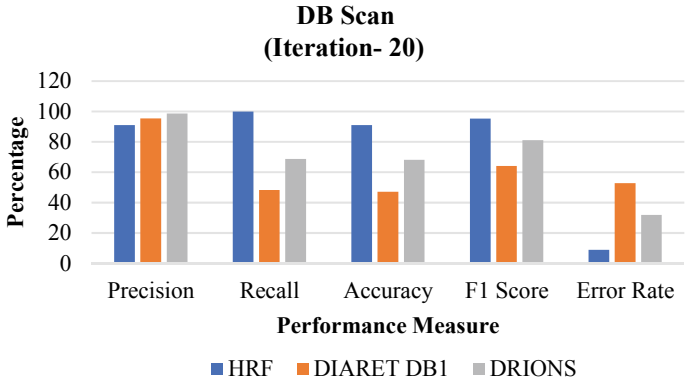

Fig. 27 Performance of DBSCAN clustering techniques with 20 iterations

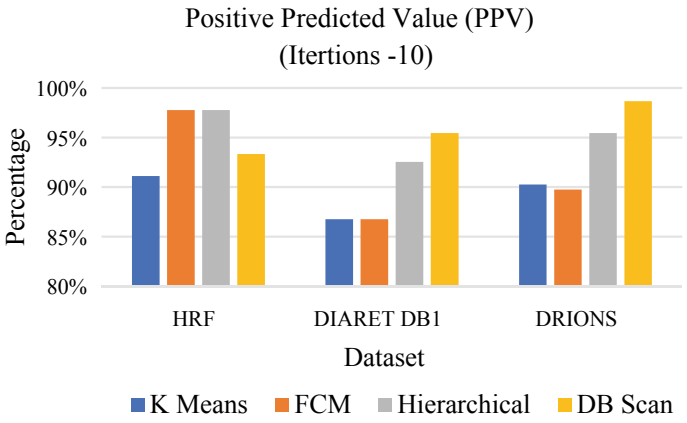

Fig. 28 Positive predicted values of clustering techniques on DRIONS, DIARETDB1 and HRF dataset for 10 iterations

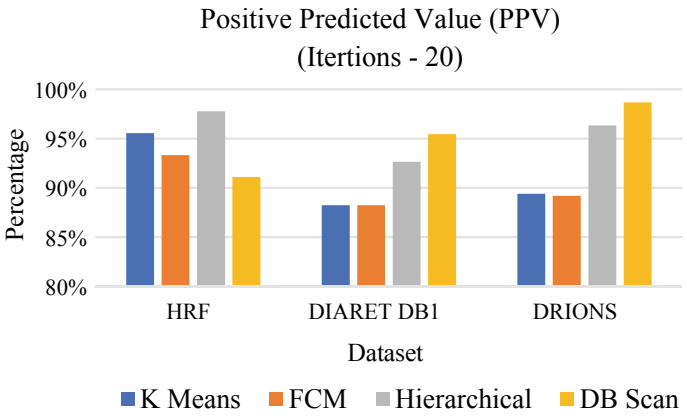

Fig. 29 Positive predicted values of clustering techniques on DRIONS, DIARETDB1 and HRF dataset for 20 iterations

The False Discovery Rate of the clustering algorithms on all the three datasets are determined and is tabulated below. Figures 30 and 31 illustrate that the probability of negatively predicted values is healthier in hierarchical clustering on HRF dataset and DBSCAN clustering for DIARETDB1 and DRIONS dataset by considering it for both 10 and 20 iterations respectively.

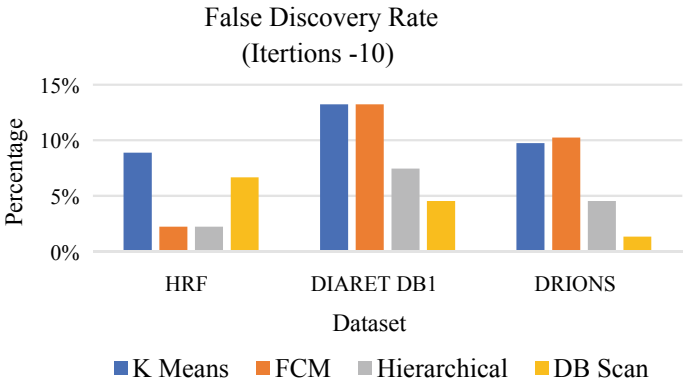

Fig. 30 False discovery rate of clustering techniques on DRIONS, DIARETDB1 and HRF dataset for 10 iterations

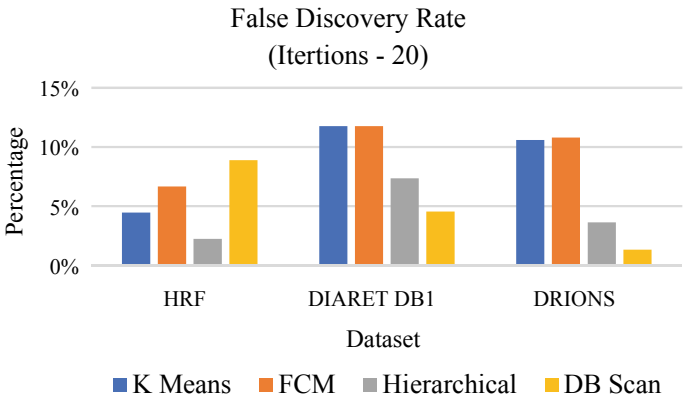

Fig. 31 False discovery rate of clustering techniques on DRIONS, DIARETDB1 and HRF dataset for 20 iterations

6 Conclusion

In this chapter the localization of optic disc is performed on the fundus images obtained from three dataset namely High-Resolution Fundus, DIARETDB1 and DRIONSDB for the iterations 10 and iteration 20 using the unsupervised learning clustering methods like DB Scan clustering, Hierarchical clustering, Fuzzy C Means clustering and K-Means clustering. The results implied that the accuracy of clustering techniques is higher on HRF dataset. Also, it is determined that Precision, Recall, F1 Score of clustering techniques on HRF dataset is better than DIARETDB1 dataset and DRIONSDB dataset for both 10 iterations and 20 iteration. The Positive Predicted Value and False Discovery Rate obtained are also found that the performance of HRF dataset is better than other two datasets. The experimentation results inferred that

the clustering techniques on HRF dataset is better when compared to DIARETDB1 and DRIONS dataset. In the future work, the localization of optic disc can also be carried out in a much more efficient way with the help of metaheuristic optimization techniques like Firefly Algorithm, Ant Colony optimization, Genetic algorithms, Differential evolution, etc.,

References

1. Jonas, J.B., Gusek, G.C., Naumann, G.O.: Optic disc, cup and neuro retinal rim size, configuration and correlations in normal eyes. Invest. Ophthalmol. Vis. Sci. **29**(7), 1151–1158 (1988)
2. Marrugo, Andrés, Millán, María: Optic disc segmentation in retinal images. Optica Pura Aplicada **43**, 79–86 (2010)
3. Kusuma Whardana, A., Suciati, N.: A simple method for optic disk segmentation from retinal fundus image. Int. J. Image Graph. Signal Process. **6**(11), 36–42 (2014). https://doi.org/10.5815/ijigsp.2014.11.05
4. Vinoth Kumar, B., Karpagam, G., Zhao, Y.: Evolutionary algorithm with Memetic search capability for optic disc localization in retinal fundus images. Intell. Data Anal. Biomed. Appl. 191–207 (2019). https://doi.org/10.1016/b978-0-12-815553-0.00009-4
5. Wang, L., Liu, H., Zhang, J., Chen, H., Pu, J.: Automated segmentation of the optic disc using the deep learning. Med. Imaging: Image Process. (2019). https://doi.org/10.1117/12.2510372
6. Edupuganti, V.G., Chawla, A., Kale, A.: Automatic optic disk and cup segmentation of fundus images using deep learning. In: 2018 25th IEEE International Conference on Image Processing (ICIP) (2018). https://doi.org/10.1109/icip.2018.8451753
7. Sharma, N., Verma, D.A.: Segmentation and Detection of Optic Disc Using Kmeans Clustering (2015)
8. Khalid, N.E., Noor, N.M., Ariff, N.M.: Fuzzy C-means (FCM) for optic cup and disc segmentation with morphological operation. Procedia Comput. Sci. **42**, 255–262 (2014). https://doi.org/10.1016/j.procs.2014.11.060
9. Lupascu, C.A., Tegolo, D., Rosa, L.D.: Automated detection of optic disc location in retinal images. In: 2008 21st IEEE International Symposium on Computer-Based Medical Systems (2008). https://doi.org/10.1109/cbms.2008.15
10. Youssif, A.A., Ghalwash, A.Z., Ghoneim, A.A.: Optic disc detection from normalized digital fundus images by means of a vessels' direction matched filter. IEEE Trans. Med. Imaging **27**(1), 11–18 (2008). https://doi.org/10.1109/tmi.2007.900326
11. Zhu, X., Rangayyan, R.M.: Detection of the optic disc in images of the retina using the Hough transform. In: 2008 30th Annual International Conference of the IEEE Engineering in Medicine and Biology Society (2008). https://doi.org/10.1109/iembs.2008.4649971
12. Lu, S.: Accurate and efficient optic disc detection and segmentation by a circular transformation. IEEE Trans. Med. Imaging **30**(12), 2126–2133 (2011). https://doi.org/10.1109/tmi.2011.2164261
13. Welfer, D., Scharcanski, J., Kitamura, C.M., Dal Pizzol, M.M., Ludwig, L.W., Marinho, D.R.: Segmentation of the optic disk in color eye fundus images using an adaptive morphological approach. Comput. Biol. Med. **40**(2), 124–137 (2010). https://doi.org/10.1016/j.compbiomed.2009.11.009
14. Yin, F., Liu, J., Ong, S.H., Sun, Y., Wong, D.W., Tan, N.M., Cheung, C., Baskaran, M., Aung, T., Wong, T.Y.: Model-based optic nerve head segmentation on retinal fundus images. In: 2011 Annual International Conference of the IEEE Engineering in Medicine and Biology Society (2011). https://doi.org/10.1109/iembs.2011.6090724

15. Cheng, J., Liu, J., Wong, D.W., Yin, F., Cheung, C., Baskaran, M., Aung, T., Wong, T.Y.: Automatic optic disc segmentation with peripapillary atrophy elimination. In: 2011 Annual International Conference of the IEEE Engineering in Medicine and Biology Society (2011). https://doi.org/10.1109/iembs.2011.6091537
16. Tjandrasa, H., Wijayanti, A., Suciati, N.: Optic nerve head segmentation using Hough transform and active contours. TELKOMNIKA (Telecommun. Comput. Electron. Control), **10**(3), 531 (2012). https://doi.org/10.12928/telkomnika.v10i3.833
17. Fraga, A., Barreira, N., Ortega, M., Penedo, M.G., Carreira, M.J.: Precise segmentation of the optic disc in retinal fundus images. In: Computer Aided Systems Theory—Eurocast 2011: 13th International Conference, Las Palmas de Gran Canaria, Spain, February 6–11, 2011, revised selected papers, pp. 584–591. Springer (2012)
18. Zhang, D., Yi, Y., Shang, X., Peng, Y.: Optic disc localization by projection with vessel distribution and appearance characteristics. In: 21st International Conference on Pattern Recognition (ICPR 2012) November 11–15, 2012. Tsukuba, Japan, pp. 3176–3179 (2012)
19. Sathya, B., Manavalan, R.: Image segmentation by clustering methods: performance analysis. Int. J. Comput. Appl. **29**(11), 27–32 (2011). https://doi.org/10.5120/3688-5127
20. Ayub, J., Ahmad, J., Muhammad, J., Aziz, L., Ayub, S., Akram, U., Basit, I.: Glaucoma detection through optic disc and cup segmentation using K-mean clustering. In: 2016 International Conference on Computing, Electronic and Electrical Engineering (ICE Cube) (2016). https://doi.org/10.1109/icecube.2016.7495212
21. Wang, W., Zhang, Y., Li, Y., Zhang, X.: The global fuzzy C-means clustering algorithm. In: 2006 6th World Congress on Intelligent Control and Automation (2006). https://doi.org/10.1109/wcica.2006.1713041
22. Hamednejad, G., Pourghassem, H.: Retinal optic disk segmentation and analysis in fundus images using DBSCAN clustering algorithm. In: 2016 23rd Iranian Conference on Biomedical Engineering and 2016 1st International Iranian Conference on Biomedical Engineering (ICBME) (2016). https://doi.org/10.1109/icbme.2016.7890942
23. Prakash, J.: Enhanced mass vehicle surveillance system. J. Res. **4**(3), 5–9 (2018)
24. Budai, A., Bock, R., Maier, A., Hornegger, J., Michelson, G.: Robust vessel segmentation in fundus images. Int. J. Biomed. Imaging **2013**, 1–11 (2013). https://doi.org/10.1155/2013/154860
25. Kauppi, T., Kalesnykiene, V., Kamarainen, J., Lensu, L., Sorri, I., Raninen, A., Voutilainen, R., Uusitalo, H., Kalviainen, H., Pietila, J.: The DIARETDB1 diabetic retinopathy database and evaluation protocol. Proc. Br. Mach. Vis. Conf. (2007). https://doi.org/10.5244/c.21.15
26. Carmona, E.J., Rincon, M., Garcia-Feijoo, J., Martinez-de-la-Casa, J.M.: Identification of the optic nerve head with genetic algorithms. Artif. Intell. Med. **43**(3), 243–259 (2008)
27. Almazroa, A., Burman, R., Raahemifar, K., Lakshminarayanan, V.: undefined. J. Ophthalmol. **2015**, 1–28 (2015). https://doi.org/10.1155/2015/180972

Mr. J. Prakash working as an Assistant Professor in the department of Computer Science & Engineering at PSG College of Technology, Coimbatore. He was born at Coimbatore in Tamil Nadu. He joined BE Compute Science & Engineering at Hindustan Institute of Technology, Coimbatore and received his UG degree on BE Computer Science & Engineering from Anna University Chennai in 2012. He also completed his ME Software Engineering at PSG College of Technology and received his on ME Computer Science & Engineering from Anna university Chennai in 2014 and currently pursuing his Ph.D. degree from Anna University, Chennai. He completed his internship at Infosys Limited, Mysore in 2014 and joined as an assistant professor in the department of Computer Science & Engineering at PSG College of Technology, Coimbatore in 2014. He also has organized many workshops, conferences and also have participated in many technical programs organized by various Institutions around India. He has guided 5 UG project and 2 PG projects and also have mentored two batch of UG students from Assam engineering College, Guwahati.

He has published more than 10 papers in peer reviewed National/International Journals, Conferences and Book chapters. He also has organized many workshops, Conferences. His current area research interests include Digital Image processing, Evolutionary Techniques.

Dr. B. Vinoth Kumar was born in Tamil Nadu, India, in 1981. He received the B.E. degree in Electronics and Communication Engineering from the Periyar University, Tamil Nadu in 2003, and the ME and Ph.D. degrees in Computer Science and Engineering from the Anna University, Tamil Nadu, India, in 2009 and 2016, respectively. In 2004, he joined the Department of Computer Science and Engineering, PSG College of Technology, Coimbatore, as a Lecturer, and in 2010 became an Assistant Professor. Since June 2018, he has been with the Department of Information Technology of the same college, as an Associate Professor. His current research interests include Computational Intelligence, Memetic Algorithms and Digital Image Processing. He has established an Artificial Intelligence Laboratory (AIR Lab) at PSG College of Technology. He is a Life Member of the Institution of Engineers-India (IEI), International Association of Engineers (IAENG) and Indian Society of Systems for Science and Engineering (ISSE). He has published papers in peer reviewed National/International Journals and Conferences and a Reviewer of International Journals.